Journal of Applied Geophysics 112 (2015) 52–61

Contents lists available at ScienceDirect

Journal of Applied Geophysics

journal homepage: www.elsevier.com/locate/jappgeo

Seismic facies analysis based on self-organizing map and empirical mode decomposition

Hao-kun Du [a,b,*], Jun-xing Cao [a,b], Ya-juan Xue [a,b,c], Xing-jian Wang [a,b]

[a] State Key Laboratory of Oil and Gas Reservoir Geology and Exploitation, Chengdu University of Technology, Chengdu 610059, China
[b] School of Geophysics, Chengdu University of Technology, Chengdu 610059, China
[c] School of Communication Engineering,Chengdu University of Information Technology,Chengdu 610225, China

ARTICLE INFO

Article history:
Received 3 June 2014
Accepted 9 November 2014
Available online 15 November 2014

Keywords:
Neural networks
SOM
EMD
Seismic facies analysis
Seismic interpretation

ABSTRACT

Seismic facies analysis plays an important role in seismic interpretation and reservoir model building by offering an effective way to identify the changes in geofacies inter wells. The selections of input seismic attributes and their time window have an obvious effect on the validity of classification and require iterative experimentation and prior knowledge. In general, it is sensitive to noise when waveform serves as the input data to cluster analysis, especially with a narrow window. To conquer this limitation, the Empirical Mode Decomposition (EMD) method is introduced into waveform classification based on SOM. We first de-noise the seismic data using EMD and then cluster the data using 1D grid SOM. The main advantages of this method are resolution enhancement and noise reduction. 3D seismic data from the western Sichuan basin, China, are collected for validation. The application results show that seismic facies analysis can be improved and better help the interpretation. The powerful tolerance for noise makes the proposed method to be a better seismic facies analysis tool than classical 1D grid SOM method, especially for waveform cluster with a narrow window.

1. Introduction

The key to reservoir modeling is the effective evaluations of rock properties and accurate mapping of their heterogeneity. Various types of information, including core samples, well logs, production data, seismic data, and geological setting, are used in this model building (de Matos et al., 2007; Rezaee, 2002). Due to the heavy cost of drilling, there is usually no adequate number of wells to build the model for relatively large areas. Specifically, data from well logs and cores only represents local properties of the reservoir and it is unreliable to extrapolate these properties to the whole prospect with the absence of enough wells. In this case, 3D seismic data plays an important role in identifying the lateral changes of reservoirs and describing their geological features. Changes in lithology, porosity, and fluid content lead to changes in amplitude, frequency, lateral continuity and other seismic attributes (de Matos et al., 2007). Thus, if changes of seismic parameters can be identified and interpreted, some valuable information of reservoirs may be extracted and may help in the understanding of subsurface geology.

Seismic facies analysis aims to interpret the variations of seismic response parameters. The so-called seismic facies can be defined as groups of seismic traces; members of the same group possess similar wave sharp. They can be viewed as the manifestation of specific sedimentary facies or geologic bodies in seismic data (John et al., 2008). So far there have been several methods and techniques of pattern recognition applied to the classification of seismic facies with varying degrees of success (e.g., Jin et al., 2007; Li and Castagna, 2004; Saggaf et al., 2003). When the geological information is unavailable, unsupervised pattern classification has been demonstrated as a powerful method for seismic facies analysis (de Matos et al., 2007). The self-organizing map (SOM) (Kohonen, 2001) is certainly one of the most successful neural network algorithms applied to unsupervised classification (e.g., Roy et al., 2010, 2012; Singh et al., 2004; Taner et al., 2001).

Seismic waveform and attribute values are the most commonly used inputs to the classification process. Since the seismic waveform contains integrated information of multiple attributes such as amplitude, frequency and phase, it is more reliable to use this integrated data directly to analysis and classification (Singh et al., 2004). However, there also exist some unnecessary information such as noise and insensitive parameters to changing geologic structure in seismic waveform. Therefore, when we use seismic waveform as the input for classification, the outcomes are generally more susceptible to noise and lower in resolution. When we use attributes values as the input, if appropriate attributes can be extracted from seismic waveform to serve as the input, the results of classification may provide higher resolution and lower amount of noise (Kuroda et al., 2012). However, the seismic attributes selection is a difficult problem and requires utmost care because

* Corresponding author at: State Key Laboratory of Oil and Gas Reservoir Geology and Exploitation, Chengdu University of Technology, Chengdu 610059, China.
E-mail addresses: dhk20052005@163.com (H. Du), caojx@cdut.edu.cn (J. Cao), xueyj0869@163.com (Y. Xue), wangxj@cdut.edu.cn (X. Wang).

http://dx.doi.org/10.1016/j.jappgeo.2014.11.007
0926-9851/

of its evident effect on the result of classification (Raeesi et al., 2012). There is no criterion for the selection of which attributes can best represent the changes in rock property (Coléou et al., 2003). This leads to more uncertainty about whether the seismic attributes we used are the optimal one to the local structural feature and what is the relationship between them. Therefore how to enhance the accuracy of SOM clustering while preserving its reliability has been a research topic in seismic facies analysis.

Seismic data volumes are significantly noisy and greatly redundant. The classification can be greatly optimized by using appropriate preprocessing on seismic data (Coléou et al., 2003). de Matos et al. (2007) applied time-frequency techniques to the SOM clustering by using the WTMMLA curves derived from trace singularities as the input data. Saraswat and Sen (2012) employed Artificial Immune System (AIS) to the compaction of seismic data and use the reduced data for SOM processing. Both of them focus on the reprocessing of seismic data in order to obtain an excellent input to the SOM clustering.

Empirical Mode Decomposition (EMD), as a new decomposition method for analyzing nonlinear and non-stationary data introduced by Huang et al. (1998), has been increasingly used for seismic signals analysis and demonstrated great potential in this application. (e.g., Battista et al., 2007; Wen et al., 2009; Xue et al., 2013, 2014). In this method, complicated seismic signals can be decomposed into a series of Intrinsic Mode Functions (IMFs) in the temporal domain (Xue et al., 2014). In essence, this decomposition method can be considered as a dyadic filter bank that serves a similar function to wavelet transform (Flandrin et al., 2004). But unlike wavelet transform required for pre-set base function, it is an adaptive data-driven method based on the local characteristic of data in time scale. Therefore, EMD method offers some distinct advantages over wavelet transform used for noise reduction and resolution enhancement of seismic data (Battista et al., 2007; Ehrhardt et al., 2012; Huang et al., 2011; Xue et al., 2013).

In this study, we introduce EMD method into unsupervised seismic facies analysis based on SOM. The seismic signals are decomposed by EMD to obtain the featured subsignals reconstructed by a number of IMFs that highlight the fine details and smooth noise. This step is to remove spikes, reduce noise and improve resolution of seismic data. Then, the reconstructed seismic subsignals are allowed as the input to SOM clustering and the useful geological information can be extracted from the results of clustering. In this paper, we will first introduce the concept of SOM and EMD, and then test our method on synthetic and real data.

2. Principle and methods

2.1. Empirical Mode Decomposition (EMD)

EMD aims to obtain IMF which is a monofrequency signal. Thus IMF has well-behaved Hilbert transforms and the physical meaning. Each IMF is defined to meet the following conditions (Huang et al., 1998):

(1) The number of zero-crossings and extrema is the same;
(2) The mean value of the upper envelops and the lower envelops is equal to zero.

EMD is carried out by a sifting process. The decomposition of a signal into IMFs by EMD is performed as follows:

1. Find out the maxima and the minima of the original signal.
2. Construct the upper envelops and the lower envelops of the signal. Generally the cubic spline method is used.
3. Obtain the mean values by averaging the upper and the lower envelopes.
4. Subtract the mean values from the original signal. Ideally, the first IMF component is produced. If the signal obtained by subtracting the mean values from the original signal does not meet the IMF condition, repeat the steps 1–4 to this signal until the first IMF component is obtained.
5. Subtract the first IMF component from the original signal and carry out the steps 1–4 to the residual component until all the IMFs are obtained.

After decomposition, the original signal can be expressed as a sum of IMFs and the residual component which is usually a monotonic function.

From the sifting process of EMD, we can find that the different IMF has different frequency ranges and probably highlights different details. For seismic data, the subsignal reconstructed by the selected IMFs which is the main component of the original seismic signal can highlight the fine details and reduce the noise.

2.2. Classification using SOM and EMD

Seismic facies analysis is an efficient measure of predicting the underlying structure and depositional environment by recognizing and analyzing the characteristics of a group of seismic reflections. The SOM, as a type of unsupervised learning (Kohonen, 2001), has been widely used in seismic facies analysis (de Matos et al., 2007; Roy et al., 2010; Saraswat and Sen, 2012; Taner et al., 2001). The EMD method is an excellent data reconstruction algorithm that removes the noise and preserves essential features of original seismic data. In our method, we introduce the EMD method into seismic facies analysis based on SOM to obtain an enhancement.

The workflow of proposed method is illustrated in Fig. 1. We first decompose seismic data into IMFs using EMD method. Then, the IMFs which contain the fine information and smooth noise are chosen to reconstruct a new seismic data. Next, we allow the reconstructed data as the input to SOM training and clustering with different numbers of facies. Comparing the facies maps, the optimal facies number can be defined.

In this workflow, the selection of the IMFs and facies numbers should be noticed. The proper selection of IMFs usually results in a better de-noising effect on seismic data. Thus it is not hard to see that the selection of IMFs directly affects the quality of the classification based on our method. Each original seismic trace usually produces a series of IMFs. Then, we should analyze the features of the IMFs displayed as seismic sections and the correlation coefficients between each IMF and original seismic trace. The IMFs which have higher correlation coefficients and greater similarity to the original seismic trace on sections will be selected for reconstruction. The deserted IMFs tend to have low correlation and a lot of noise which is evident from the seismic sections.

The number of classes, i.e., the number of seismic facies, has important effects on the classification process and should be estimated very carefully (Raeesi et al., 2012). A low number of classes can only offer a very rough classification in which some important information may be obscured and the facies of interest usually cannot be identified. Conversely, the high number of classes can enhance details and accuracy of the classification; however, it also produces lots of redundant facies which might complicate the interpretation. In unsupervised seismic facies analysis, one can use more seismic facies than the number of expectant geofacies in the researched region (Raeesi et al., 2012). Because the additional facies could be required to represent the noise (Roy et al., 2012), including background noise and horizon interpretation noise caused by interpretation errors or time displacement, and the transition zone between the main facies. The noises are represented by one or several facies with haphazard distribution; while the transition zone's facies usually distribute along the periphery of the main facies. The best situation is that with the increasing number of classes, the main facies remain about the same and only the number of unnecessary facies is in the growth. Therefore, the estimation of the number of classes in study area requires iterative testing and prior knowledge.

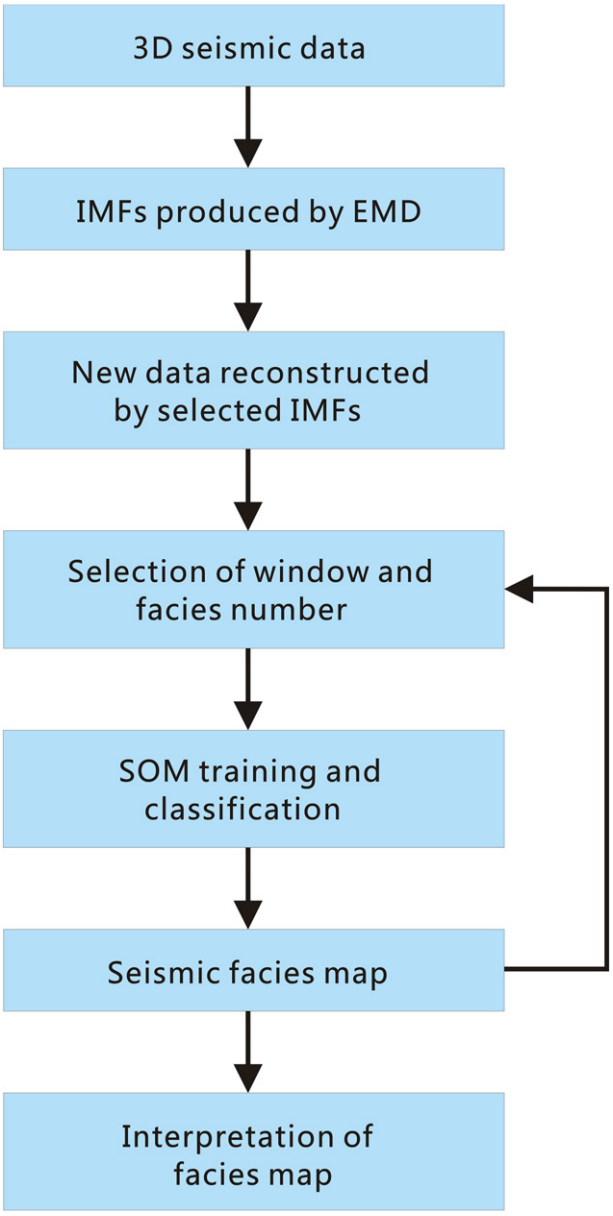

Fig. 1. Workflow of waveform classification based on SOM and EMD.

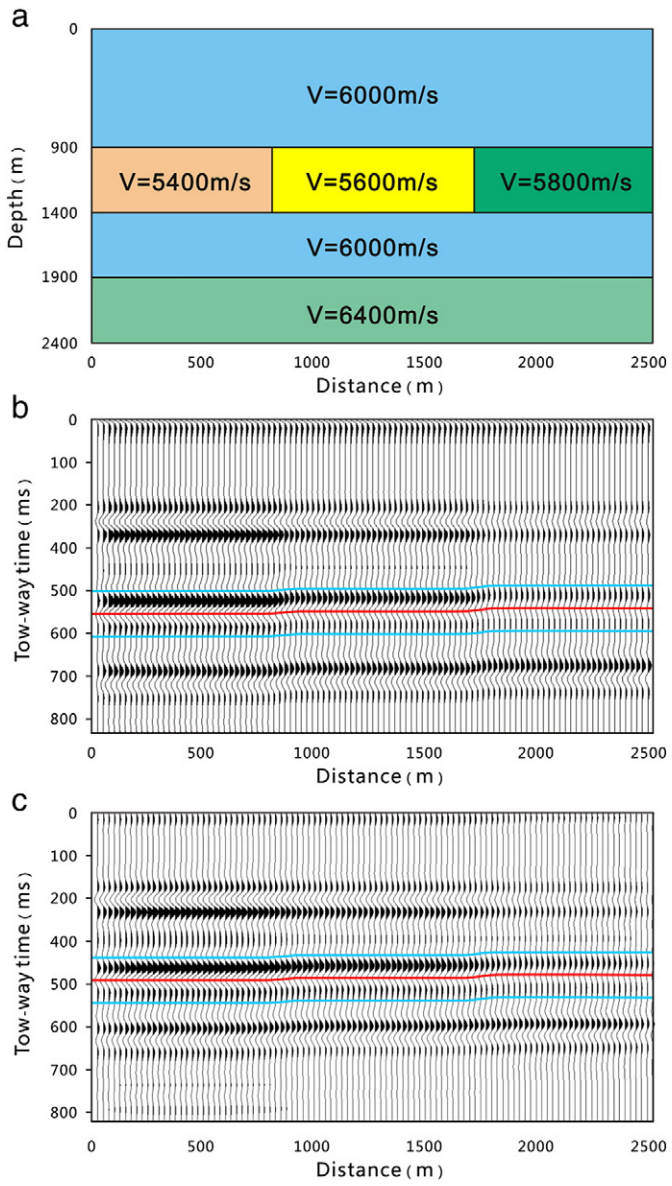

Fig. 2. Simple stratum model composed by layers with different P-wave velocity. (a) Simple carbonate system model; (b) synthetic seismic data; (c) constructed seismic data processed by EMD.

3. Synthetic data

To illustrate the effectiveness of the proposed method, we apply it in a synthetic seismic data shown in Fig. 2b, which is derived from a simple carbonate system model shown in Fig. 2a. The geofacies that we want to identify are lying in the second layer (from the top) and marked with their P-wave velocities of 5400 m/s, 5600 m/s, and 5800 m/s (Fig. 2a). Fig. 2c shows the processed section constructed by IMF2 and IMF3. Because our original synthetic section is produced in an ideal situation, the processed section does not show any improvement except removing spikes and smoothing the time displacement at the interface of velocity in target layer. Fig. 3 shows the seismic sections of the original synthetic data (a), deserted IMF1 (b) and selected IMF2 (c). Lots of noise is evident from the section of IMF1 which has a low correlation coefficient. Conversely, the section of IMF2 displays even less noise than original synthetic data and has a high correlation coefficient. In this way, we finally select the IMF2 and 3 and desert the IMF1, 4, 5 and 6.

We begin this testing by selecting a time window of 28 ms around the base of target area denoted by the red line, i.e., the zone between the blue lines show in Fig. 2b. Then the waveform classification is performed iteratively with the different numbers of classes, using the original data and the reconstructed data of the specific time window as the input respectively.

Fig. 4a, b, and c illustrate the results of the classifications for original data with the facies numbers of 3, 4, and 6; Fig. 4d, e, and f show the results from the data processed by EMD with the corresponding numbers of the facies. Fig. 4a indicates that the result of waveform classification is very sensitive to time displacement. In our synthetic, the time displacement is derived from velocity contrast of the horizontal layer. When we use three classes in seismic facies analysis which is equal to the number of predefined geofacies, only two geofacies can be identify and the time displacement occupies one of the seismic facies (Fig. 4a). When we use four classes, all the geofacies can be identify and the time displacement also occupies one of the seismic facies (Fig. 4b).

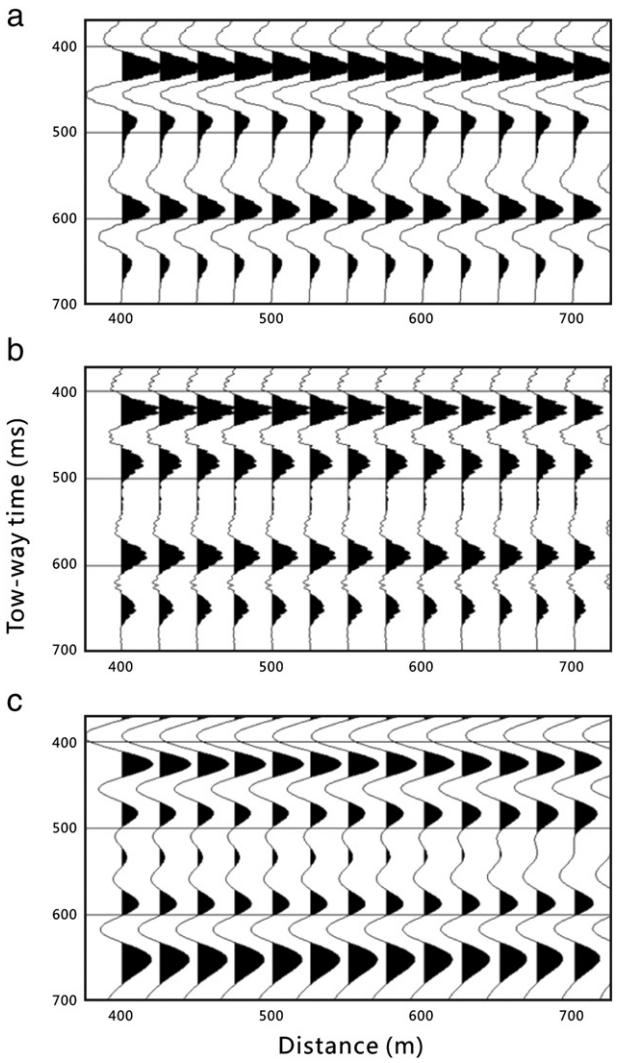

Fig. 3. Seismic sections of (a) the original synthetic data, (b) deserted IMF1 and (c) selected IMF2 (c).

The horizon interpretations of real seismic data are almost noisy and contain lots of time displacement. Therefore the additional facies are required to represent such interpretation noise in seismic facies analysis. Fig. 4c shows the seismic facies map with six classes. Compared with the facies map in Fig. 4b, we can see that the added two facies are still used to represent the interpretation noise and the noise's facies appear a little wider in Fig. 4c. Thus, it is easy to see that using excessive facies tend to result in more noise and the optimum number of the classes appears when the main facies begin to become steady with the increasing classes (four in this testing).

Comparing the facies maps on the left and the right with the same number of classes in Fig. 4, the facies maps on the right confirm better performance due to the narrower width of noise' facies, especially the one with four facies (Fig. 4e) presents a perfect effect.

This test was repeated by adding Gaussian noise to original synthetic data. Fig. 5a shows synthetic section with Gaussian noise. The IMF3, 4 and 5, which have the highest correlation coefficients with the noise section, are selected to reconstruct a new section shown by Fig. 5b. Obviously, the section processed by EMD has much less noise. Sure enough, the noise section gave a bad result of cluster analysis shown in Fig. 5c. Meanwhile, the reconstructed section provided a better result shown in Fig. 5d. The above tests confirm that our method has a good performance in the application to seismic facies analysis for synthetic data and has a good noise tolerance.

4. Application to real seismic data

We apply our method to a real 3D seismic data set from the western Sichuan basin, China (Fig. 6). This set acquisition was carried out in the NE-SW direction within an area of nearly 150 km^2. Its CMP line spacing is nearly 25 m and the recording length is 5.8 s with 2 ms of sampling rate. The dominant frequency of target zone is about 28Hz. There are three wells inside the survey. Well A is located in the east of the survey, well B is in the center and well C is in the west. The target geological formation is the top of Leikoupo formation in Middle Triassic. In the Middle Triassic period, the western Sichuan basin was covered by a warm, shallow sea with plentiful marine life. With the long-term regression in the late stage of Middle Triassic, the carbonate rocks of most area exposed the surface and were transformed by leaching and weathering. Therefore, large scale weathering crust and karstic reservoirs were

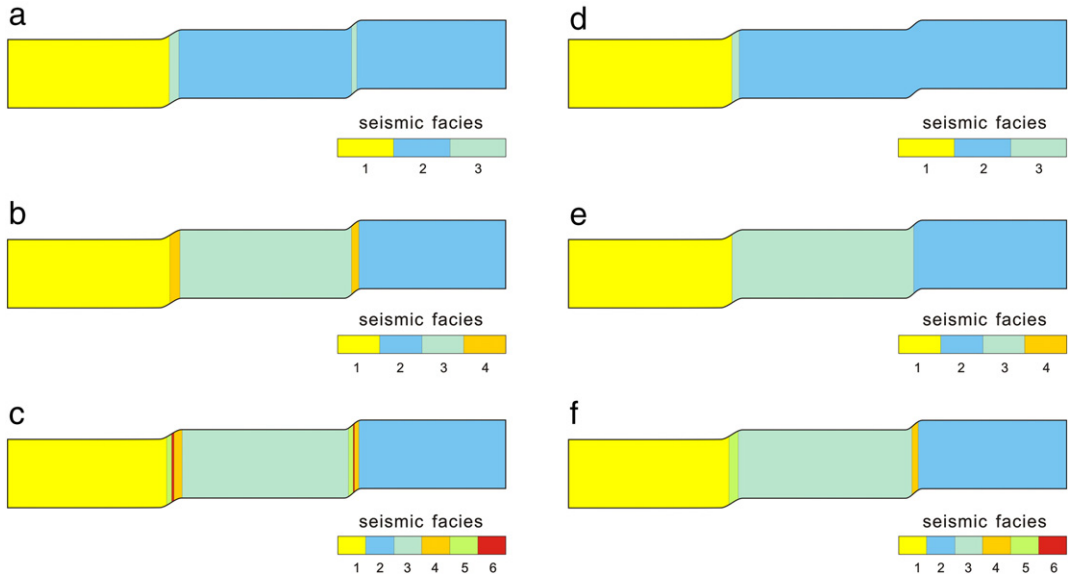

Fig. 4. Facies maps of synthetic seismic data with different facies number and input; (a), (b), and (c) facies maps with 3, 4, and 6 facies generated by using SOM alone. (d), (e), and (f) facies maps with 3, 4, and 6 facies generated by using SOM and EMD.

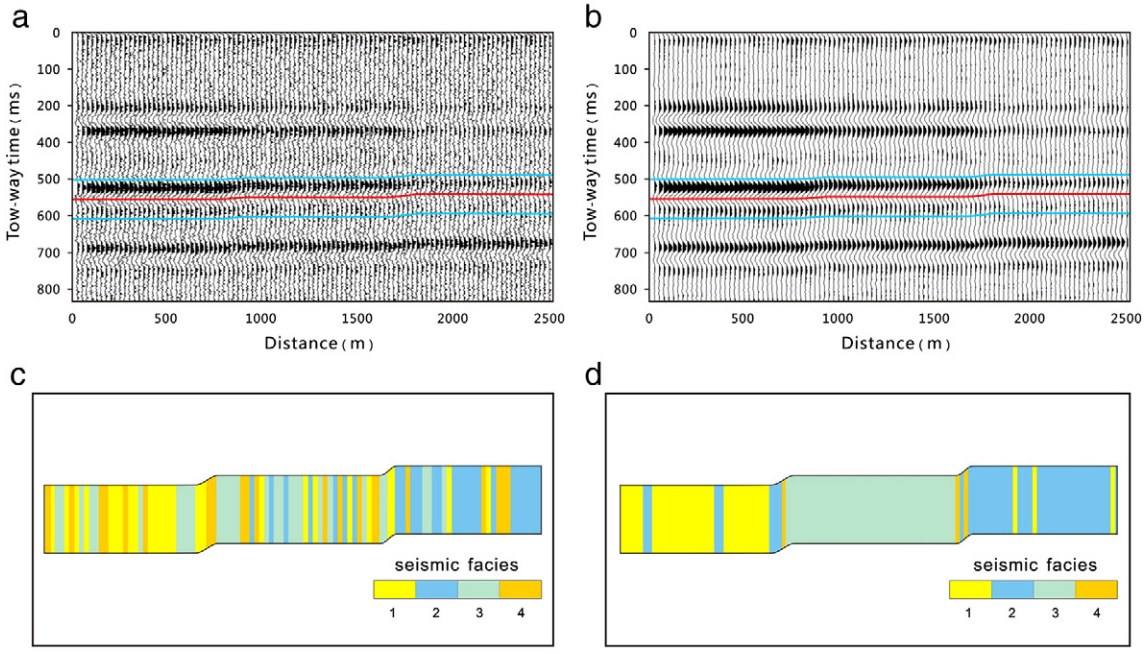

Fig. 5. (a) Synthetic model section which added the Gaussian noise to; (b) reconstructed section processed by EMD; (c) facies map of noise section; (d) facies map of reconstructed section.

widespread in this area. The weathering occurred in the study area was not intense and the weathering crust karst reservoirs was only developed in partial region. Well A and C have approximately 70–80 m of weathering crust rich zone in the top of Leikoupo formation. Unlike the dense, non-porous surrounding limestone, karstic reservoirs have relatively high porosity and lots of solution pores and cavities, accompanied by a series of high angle fractures (Fig. 7). These features of reservoirs are demonstrated clearly on the cores and logs of well A and well C. While the available cores and well logs (relatively high density and velocity) from well B give an indication of poor weathering crust (Fig. 8).

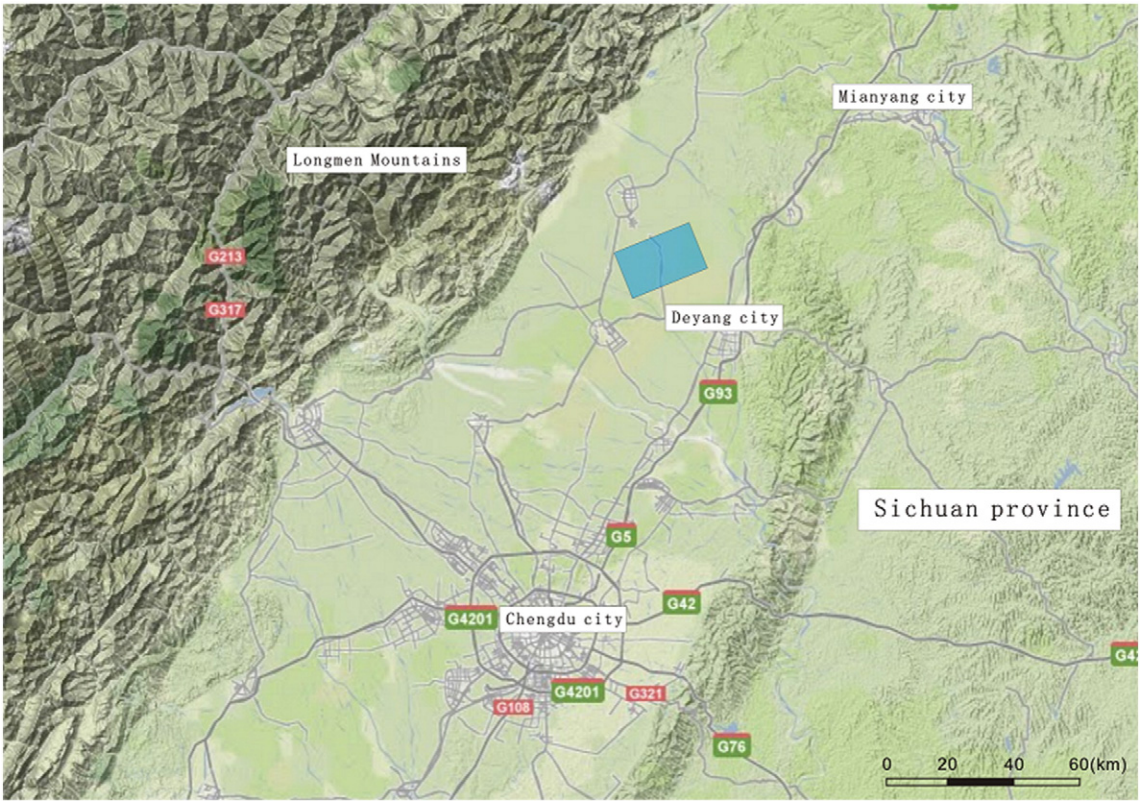

Fig. 6. Map from Google Maps, with blue area marking the location of the field covered by 3D seismic data set.

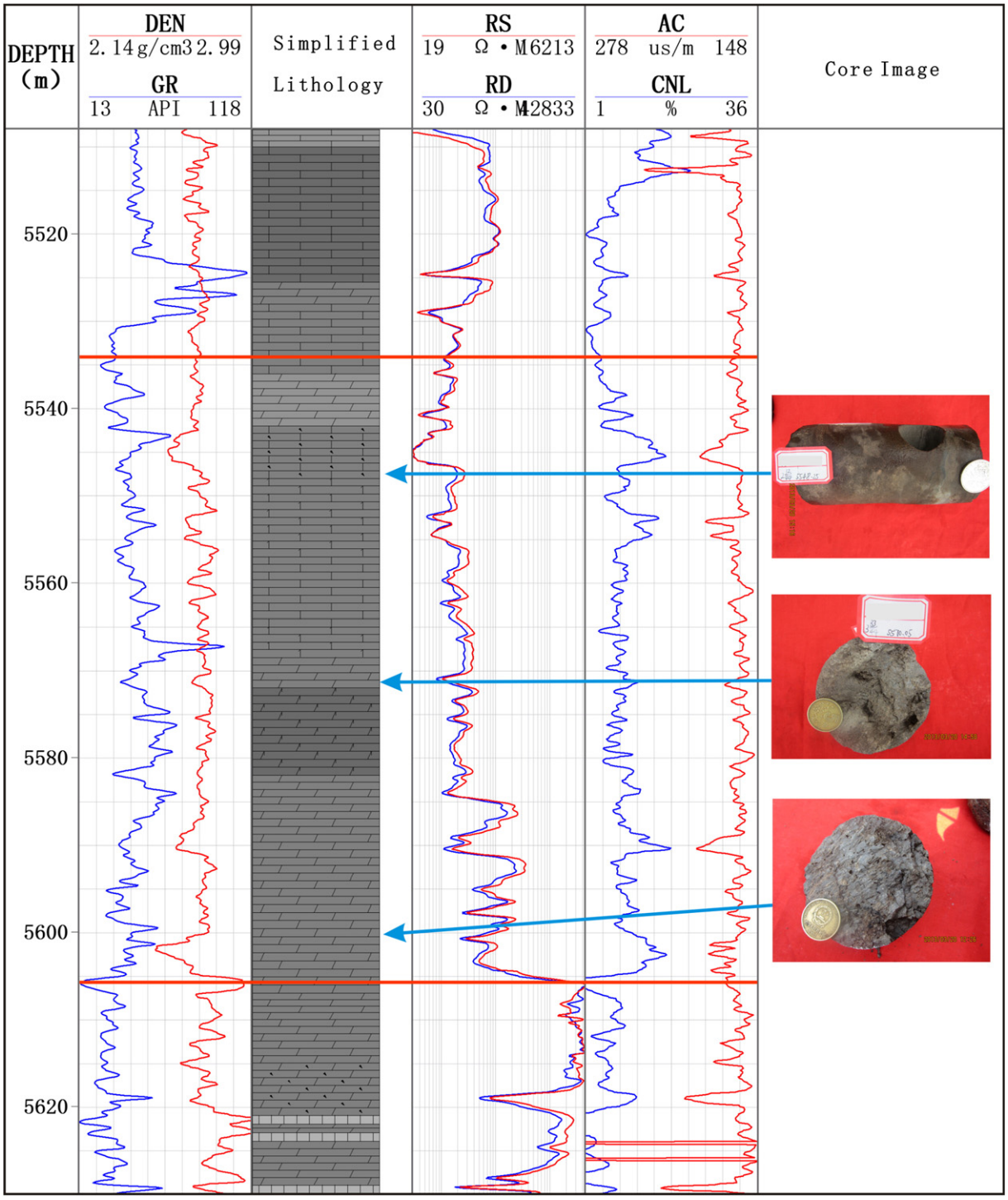

Fig. 7. General stratigraphic column of well A. Region of Interest is between the red lines. Solution pores and cavities are clearly present in photos.

We intend to map the weathered crust area which is favorable for reservoir development using EMD-based SOM methods. The weathering crust rich formation in study area has a big variation of lateral thickness due to the differences of weathering intensity. The thickness is about 10–80 m down from the top of Leikoupo formation. Therefore we intend to use the top of Leikoupo formation, i.e., reservoir top to limit the time window. It will be selected in ranges from 0 ms to 10 ms (about 30 m in depth domain) beneath the reservoir top. Fig. 9 (section A) shows the seismic section intersecting known wells and the top (yellow line) and base (blue line) of interpreted karst reservoir. The seismic event, that represents the reservoir top and the surface of unconformity, presents excellent lateral continuity and stability; its horizon interpretation has high reliability and low noise.

Each original seismic trace will produce about six to seven IMFs. By analysis, the main components of the original seismic trace are reflected in the first three IMFs. Therefore, the first three IMFs of the original seismic volume are selected for reconstruction. The method of the IMFs selection is mentioned above and more details can be found in Xue et al. (2013, 2014). Additionally, this process will not change the size of the original data set. Fig. 9 shows the same seismic random

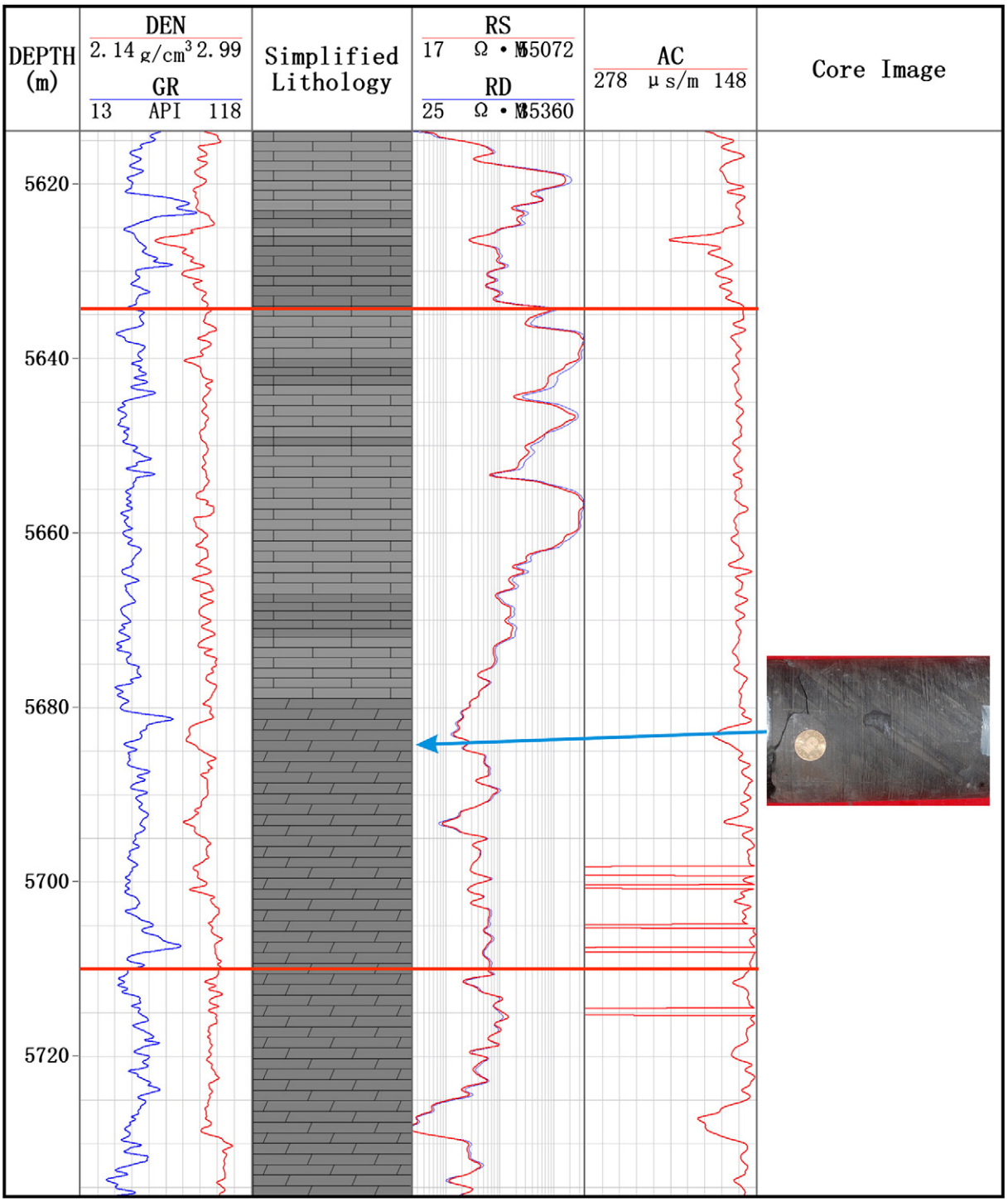

Fig. 8. General stratigraphic column of well B. Region of Interest is between the red lines. Photo shows the core of compact limestone.

lines intersecting known wells from original seismic data (section A) and the data processed by EMD (section B). From Fig. 9, we can see that section B preserves the main features of section A and has a clearer distinction between events both in horizontal and vertical direction. This is useful for waveform cluster analysis to suppress the interference of noise.

The facies map is not the end product interpretation. We should transform seismic facies map into geofacies map based on well constraint, depositional setting, and some other useful information. In this study, we first use well data to define the geofacies corresponding to seismic facies into well locates. Then section feature, ancient landform, and depositional setting are employed to verify the conclusion. Fig. 10 illustrates the thickness between karst reservoir top and base. For a plain restricted platform under weathering action, the smaller sedimentary thickness is usually caused by weathering and denudation. This can be used to verify the reliability of the results of the classification.

We clustered our seismic data set with four classes, because the main facies still remained about the same if we used classes over 4.

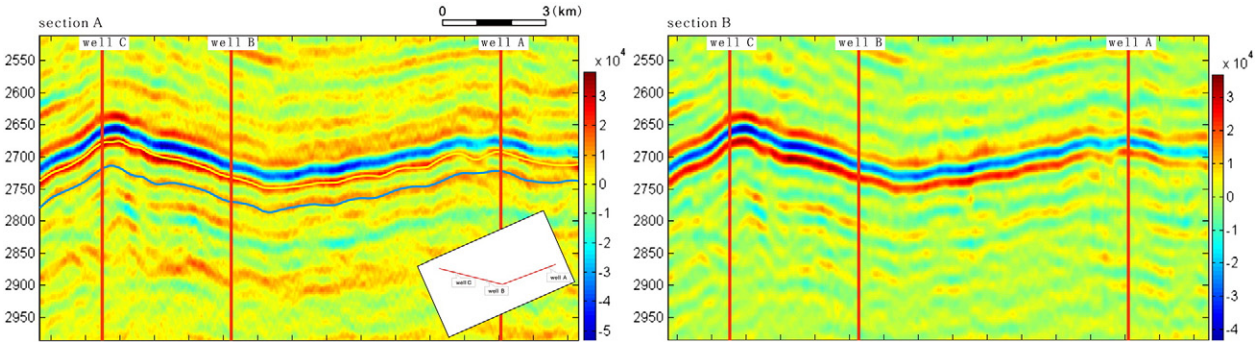

Fig. 9. Section A is a through-well seismic line from real seismic data. The yellow line denotes the reservoir top interpretations and blue line denotes the base. The base map in the lower-right corner shows the location of the line. Section B is the same line processed by EMD.

Fig. 11 shows the results of seismic facies analysis with a time windows of 10 ms beneath the reservoir top. Fig. 11a illustrates the results of the classifications for original data; Fig. 11b shows the results from the data processed by EMD. It can be observed in Fig. 11 that well A and C whose cores have the obvious characteristics of weathered crust fall in the areas occupied by facies numbers 1 and 2 (numbers written on the right side of the color bar). From seismic point of view, some reflectors of these areas present lower energy, weak continuity and up dip pinch-out which is the typical seismic facies belong to weathering crust shown in Fig. 12. Additionally, there is a great similarity between the distributions of these areas and the small thickness regions shown in Fig. 10 (warm colors). Therefore, facies numbers 1 and 2 are proved to indicate the weathering crust areas. The events of the facies No. 3 present excellent lateral continuity and higher energy (Fig. 12). These are typical seismic features of tidal flat, so we speculate that facies No. 3 denotes the tidal flat. From the core of well B, we learn that facies No.4 indicates the lagoon of restricted platform.

Fig. 11a shows the low resolution and strong presence of noise. It provides a rough result of classification from which the boundary of seismic facies is hardly identifiable. In contrast, the facies map showed in Fig. 11b is better in the delimitation of the seismic facies because of the lower amount of noise. The faults and three main facies aforementioned can be easily identified from the latter map. More importantly the distributions of facies No. 1 and 2 in Fig. 11b present a better similarity to the small thickness regions shown in Fig. 10. This shows that the enhancement of our method is reliable for real seismic. By comparison, our method can be demonstrated to have an outstanding performance in noise reduction and resolution enhancement with the presupposition of high reliability.

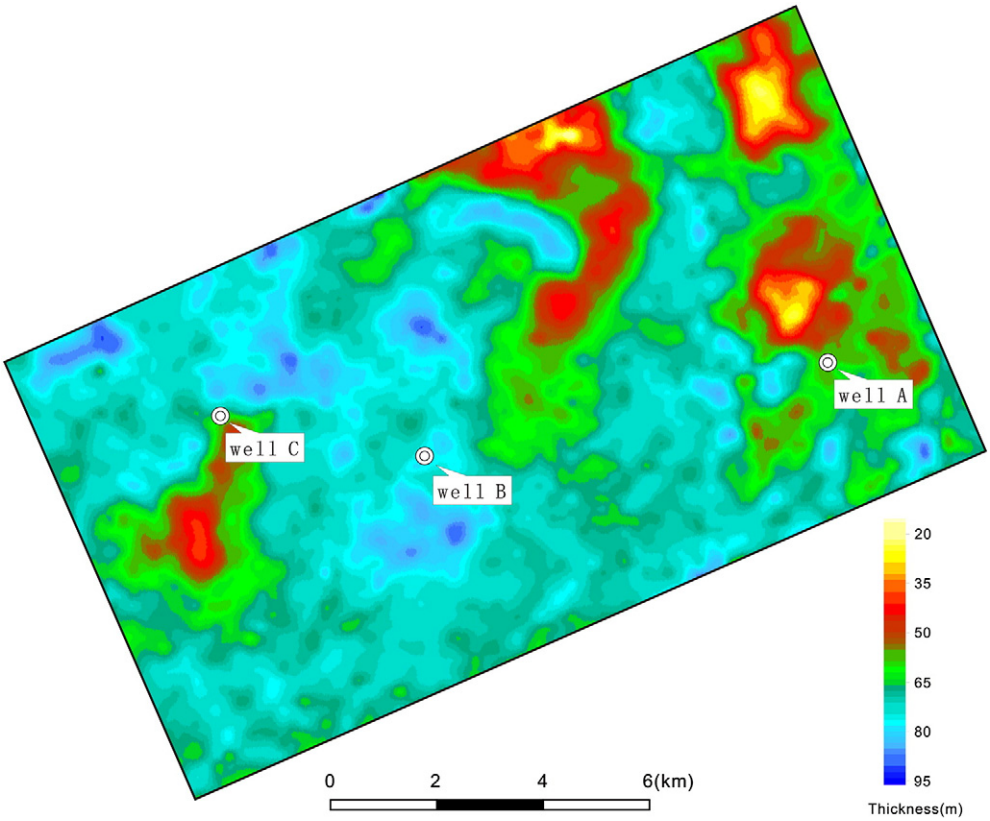

Fig. 10. Thickness of the reservoir.

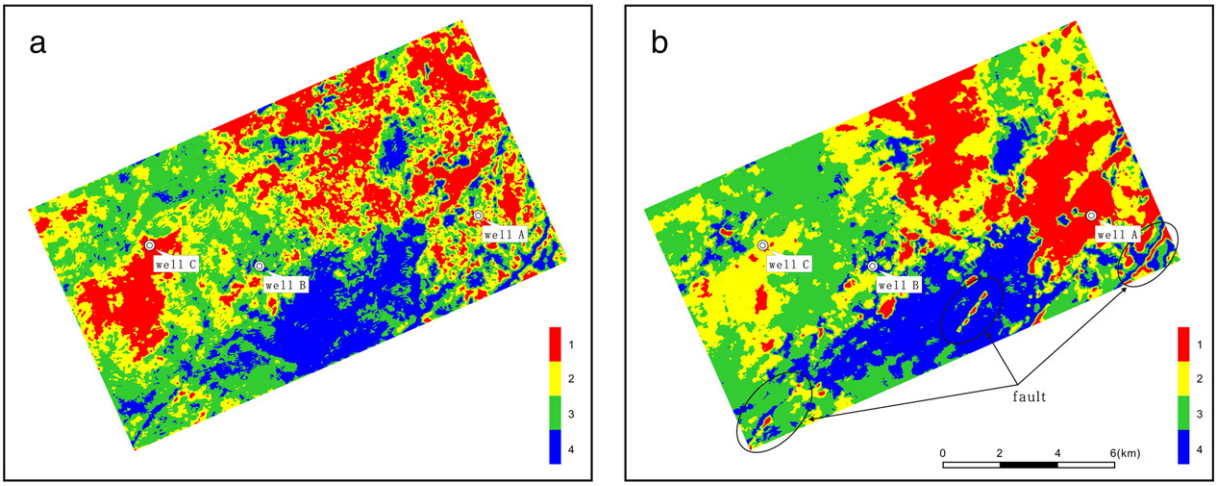

Fig. 11. Facies maps of real seismic data with different inputs. (a) Facies maps from original seismic data. (b) Facies maps from reconstructed seismic data using EMD.

5. Conclusion

The EMD-based SOM method is discussed for waveform classification. The seismic subsignals are reconstructed by the selected IMFs which reflect the main information of the original signal and contain more fine details and less noise. Thus reconstructed data set from EMD processing preserves main feature of the original seismic set. Moreover, the computing speed of this process is very fast. Model test and application of the proposed method to real seismic data from western Sichuan basin, China show that the proposed method has better effects in waveform classification than the standard SOM method does. It can be seen from the comparison of the results that the traditional waveform clustering used SOM is susceptible to interpretation noise (time displacement) due to the phase change. This may interfere with the recognition of geofacies and geologic features such as faults and fractures. However, our proposed method is less sensitive to noise especially for waveform cluster analysis with a narrow window. It can be a powerful tool to offer a valid reference for fine reservoir description.

Acknowledgments

This study was supported by the National Natural Science Foundation of China (Grant Nos. 41430323, 41274128 and 41404102), which is greatly appreciated.

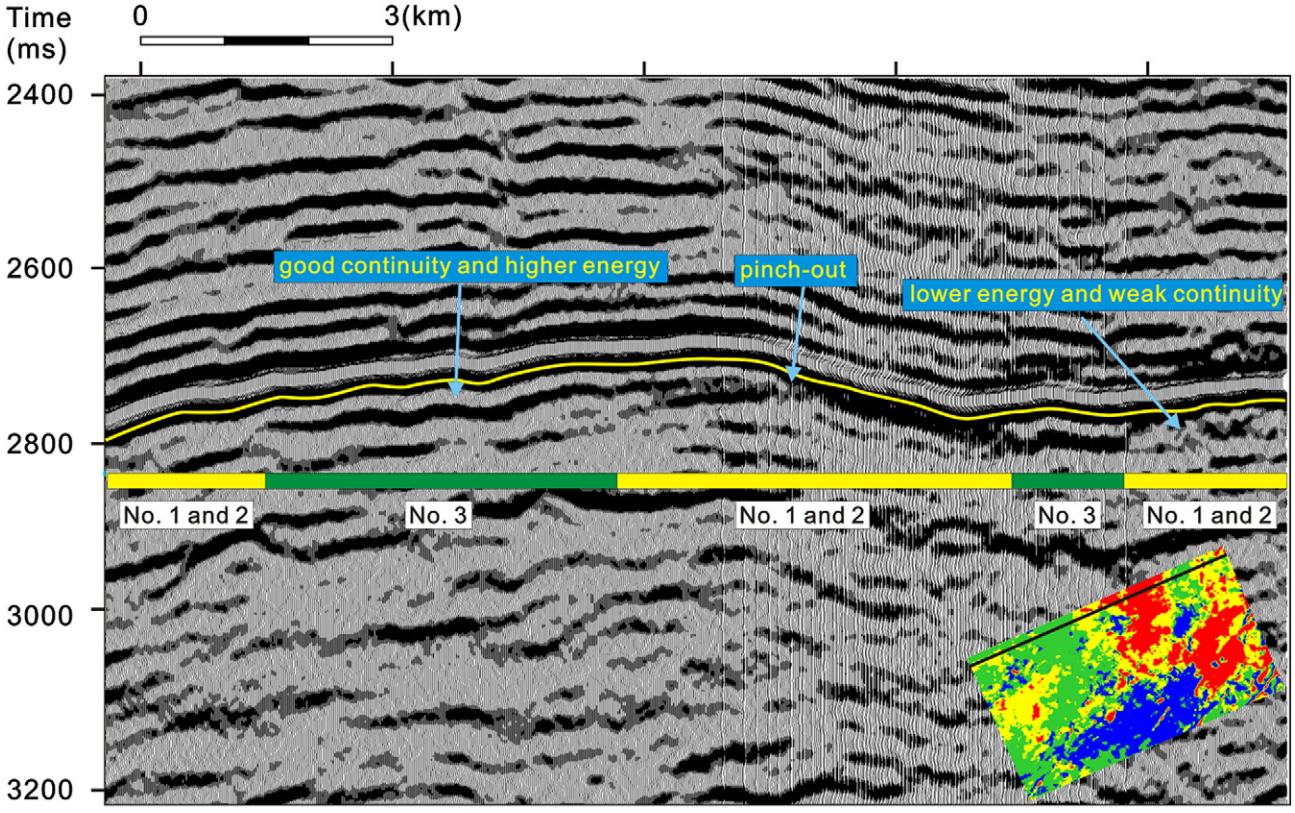

Fig. 12. Typical section features of facies.

References

Battista, B.M., Knapp, C., McGee, T., Goebel, V., 2007. Application of the empirical mode decomposition and Hilbert-Huang transform to seismic reflection data. Geophysics 72 (2), H29–H37. http://dx.doi.org/10.1190/1.2437700.

Coléou, T., Poupon, M., Azbel, K., 2003. Unsupervised seismic facies classification: a review and comparison of techniques and implementation. Lead. Edge 22 (10), 942–953. http://dx.doi.org/10.1190/1.1623635.

de Matos, M.C., Osorio, P.L., Johann, P.R., 2007. Unsupervised seismic facies analysis using wavelet transform and self-organizing maps. Geophysics 72 (1), P9–P21. http://dx.doi.org/10.1190/1.2392789.

Ehrhardt, M.J., Villinger, H., Schiffler, S., 2012. Evaluation of decomposition tools for sea floor pressure data: A practical comparison of modern and classical approaches. Comput. Geosci. 45, 4–12. http://dx.doi.org/10.1016/j.cageo.2012.03.022.

Flandrin, P., Rilling, G., Goncalves, P., 2004. Empirical mode decomposition as a filter bank. Signal Process. Lett. IEEE 11 (2), 112–114. http://dx.doi.org/10.1109/LSP.2003.821662.

Huang, N.E., Shen, Z., Long, S.R., Wu, M.C., Shih, H.H., Zheng, Q., Liu, H.H., 1998. The empirical mode decomposition and the Hilbert spectrum for nonlinear and non-stationary time series analysis. Proc. R. Soc. Lond. Ser. A Math. Phys. Eng. Sci. 454 (1971), 903–995. http://dx.doi.org/10.1098/rspa.1998.0193.

Huang, Y.P., Geng, J.H., Zhong, G.F., Guo, T.L., Pu, Y., Ding, K.Y., Ma, J.Q., 2011. Seismic attribute extraction based on HHT and its application in a marine carbonate area. Appl. Geophys. 8 (2), 125–133. http://dx.doi.org/10.1007/s11770-010-0279-z.

JanuaryJin, L., Sen, M.K., Stoffa, P.L., 2007. Fusion based classification method and its application. 2007 SEG Annual Meeting. Society of Exploration Geophysicists http://dx.doi.org/10.1190/1.2792784.

John, A.K., Lake, L.W., Torres-Verdin, C., Srinivasan, S., 2008. Seismic facies identification and classification using simple statistics. SPE Reserv. Eval. Eng. 11 (06), 984–990. http://dx.doi.org/10.2118/96577-PA.

Kohonen, T., 2001. Self-organizing maps, 3rd ed. Springer http://dx.doi.org/10.1007/978-3-642-56927-2.

Kuroda, M.C., Vidal, A.C., de Carvalho, A.M.A., 2012. Interpretation of seismic multiattributes using a neural network. J. Appl. Geophys. 85, 15–24. http://dx.doi.org/10.1016/j.jappgeo.2012.06.009.

Li, J., Castagna, J., 2004. Support vector machine (SVM) pattern recognition to AVO classification. Geophys. Res. Lett. 31 (2). http://dx.doi.org/10.1016/j.jappgeo.2012.06.009.

Raeesi, M., Moradzadeh, A., Doulati Ardejani, F., Rahimi, M., 2012. Classification and identification of hydrocarbon reservoir lithofacies and their heterogeneity using seismic attributes, logs data and artificial neural networks. J. Pet. Sci. Eng. 82, 151–165. http://dx.doi.org/10.1016/j.petrol.2012.01.012.

Rezaee, M.R., 2002. Petroleum Geology. Alavi Publications (P472).

Roy, A., Marfurt, K.J., de Matos, M.C., 2010. Applying self-organizing maps of multiple attributes, an example from the Red-Fork Formation, Anadarko Basin. 2010 SEG Annual Meeting. Society of Exploration Geophysicists http://dx.doi.org/10.1190/1.3513145 (January).

Roy, A., Dowdell, B.L., Marfurt, K.J., 2012. Characterizing a Mississippian tripolitic chert reservoir using 3D unsupervised seismic facies analysis and well logs: an example from Osage County, Oklahoma. 82nd Annual International Meeting of the Society of Exploration Geophysicsts, Expanded Abstracts http://dx.doi.org/10.1190/segam2012-1365.1 (September).

Saggaf, M.M., Toksöz, M.N., Marhoon, M.I., 2003. Seismic facies classification and identification by competitive neural networks. Geophysics 68 (6), 1984–1999. http://dx.doi.org/10.1190/1.1635052.

Saraswat, P., Sen, M.K., 2012. Artificial immune-based self-organizing maps for seismic-facies analysis. Geophysics 77 (4), O45–O53. http://dx.doi.org/10.1190/geo2011-0203.1.

Singh, V.B., Subrahmanyam, D., Negi, S.P.S., Baid, V.K., Kumar, Ajai, Biswal, S., 2004. Facies classification based on seismic waveform—a case study from Mumbai high north. 5th Conference & Exposition on Petroleum Geophysics.

Taner, M.T., Walls, J.D., Smith, M., Taylor, G., Carr, M.B., Dumas, D., 2001. Reservoir characterization by calibration of self-organized map clusters. SEG/San Antonio http://dx.doi.org/10.1190/1.1816406.

Wen, X., He, Z., Huang, D., 2009. Reservoir detection based on EMD and correlation dimension. Appl. Geophys. 6 (1), 70–76. http://dx.doi.org/10.1007/s11770-009-0002-5.

Xue, Y.J., Cao, J.X., Tian, R.F., 2013. A comparative study on hydrocarbon detection using three EMD-based time–frequency analysis methods. J. Appl. Geophys. 89, 108–115. http://dx.doi.org/10.1016/j.jappgeo.2012.11.015.

Xue, Y.J., Cao, J.X., Tian, R.F., 2014. EMD and Teager–Kaiser energy applied to hydrocarbon detection in a carbonate reservoir. Geophys. J. Int. 197, 277–291. http://dx.doi.org/10.1093/gji/ggt530.